

Circular Dichroism in the Photoionization of Nanoparticles from Chiral Compounds

Johannes Paul, Armin Dörzbach, and Konstantin Siegmann

Laboratory for Solid State Physics, Swiss Federal Institute of Technology (ETH), CH-8093 Zürich, Switzerland

(Received 19 March 1997)

The dichroism in photoemission from chiral molecules is observed for the first time. Particles consisting of chiral molecules are suspended in air and irradiated alternately with right and left circularly polarized uv light. We found a polarization dependence in the total photoelectric current. The asymmetries observed are of the order of 10^{-2} to 10^{-3} , as expected from perturbation theory, and reverse their sign when the handedness of the molecules is changed. [S0031-9007(97)04233-6]

PACS numbers: 33.55.Ad, 33.15.Bh, 79.60.-i, 82.70.Rr

The interaction between chiral molecules and polarized light displays optical activity [1] and was first investigated by Biot and later by Pasteur [2]. Pasteur also resolved racemic tartaric acid into the enantiomers. Today, optical rotation and circular dichroism (CD) in photoabsorption are well established tools in analytical chemistry [3]. In these techniques, the rotation of the polarization axis of the transmitted linearly polarized light or the difference in extinction coefficients for left- and right circularly polarized light is measured. Optical activity can also occur with nonchiral compounds when the experimental geometry is chiral [4]. This necessarily requires molecules which are aligned or oriented due to external (i.e., electric or magnetic fields) or internal forces (i.e., strained or stressed material, coated surfaces) [5].

In analogy to the dichroism in photoabsorption, it was predicted that the photoemission from chiral molecules should also depend on the helicity of the light [6,7]. In the angular distribution of the photoelectrons from unaligned chiral molecules, circular dichroism can occur within a pure dipole approximation theory. But in a photoemission experiment without angular resolution, dichroism occurs only in higher order approximations [7,8]. Circular dichroism in the angular distribution of the photoelectrons exists even from nonchiral compounds when the molecules are aligned or oriented in space [7,9,10]. This is caused by the chirality of the experimental geometry, due to the handed coordinate system given by the propagation direction of the light, the direction of the emitted electrons, and the orientation of the molecules. Asymmetries up to 80% are observed [10]. Recently, circular dichroism in the double photoionization of He in an angle resolved coincidence experiment was reported [11]. In this experiment the third axis of a handed coordinate system is given by the emission direction of the second photoelectron.

In order to determine the effect stemming from molecular chirality alone one has to carefully avoid chirality in the experimental setup. This is achieved in photoemission of electrons from aerosols [12,13] because nanoparticles in gas suspension (aerosol) are randomly oriented and not aligned. The photoelectrons from such particles are ther-

malized by collisions with the surrounding gas molecules [12]. The final thermalization state is independent of photoelectron properties such as spin or kinetic energy. In practice, one in fact measures the positive charge left behind on the particles after the photoelectron has been removed. Therefore, chiral geometry is strictly eliminated in this experiment. Photoemission on aerosols has the advantage that dichroic effects can arise only from the handedness of the particles or their molecular building blocks.

We chose molecules where the light absorbing part, called chromophore, is chiral. 1,1'-Binaphthyl-2,2'-diyl hydrogen phosphate has two achiral π systems which interact in a chiral way due to their geometrical arrangement (Fig. 1). Both enantiomers are commercially available in high purity (>99%). CD spectra of binaphthalene derivatives show strong dichroism in the uv range [14] which is explained by the exciton coupling model [15].

The experimental setup consists of three parts: the particle generation section, the source for polarized light, and the photoemission tube. A solution of one enantiomer of the binaphthalene in methanol (20 mg in 250 ml) is nebulized continuously yielding a stable flow of fine droplets. The solvent in these droplets is subsequently evaporated, and the dissolved compounds crystallize to form particles in the nanometer size range. These particles are polydisperse, i.e., a broad size distribution is obtained ($5 \text{ nm} < \text{diameter} < 300 \text{ nm}$). In order to generate a sharp distribution the particles are size selected in a differential mobility analyzer (DMA) [16] according to their mobility in an electric field. This technique requires a

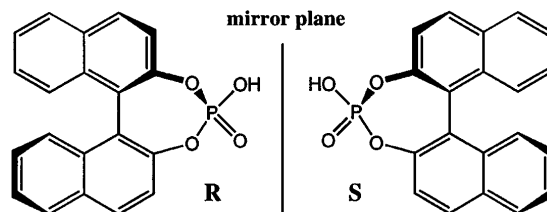


FIG. 1. The *R*- and *S*-configuration of 1,1'-binaphthyl 2,2'-diyl hydrogen phosphate. The angle between the two naphthalenes is 60° (-60° , respectively).

known charge distribution of the particles which is realized with a radioactive diffusion charger. The charge distribution is derived by the Fuchs theory [17]. More than 90% of the charged particles investigated are singly charged. In our setup only negatively charged particles within a small mobility diameter range ($\Delta d/d < 0.15$) leave the DMA and enter the photoemission tube. Typically, the particle concentration of the monodisperse aerosol is higher than 10^4 cm^{-3} . The particle size and shape is also checked by scanning electron microscopy which shows that the particles are spherical. The particle formation method used avoids heating of the chiral compound. Racemization can therefore be excluded.

In Fig. 2 the photoemission unit is shown. As the light source we use an excimer laser filled with an ArF gas mixture ($\lambda = 193.4 \text{ nm}$; pulse duration = 20 ns). The laser light is attenuated by dielectric mirrors and linearly polarized by thin film polarizers. Left and right circularly polarized light is obtained with a rotatable, single order $\lambda/4$ plate made of crystalline quartz. The degree of circular polarization [$P = (I^{\text{LCP}} - I^{\text{RCP}})/(I^{\text{LCP}} + I^{\text{RCP}})$] was determined and is greater than 99.5%. The polarized light is directed through a 30 cm long photoemission tube where the light interacts with the size selected particles. After exiting the tube, the light intensity is measured by a fluorescence detector in order to monitor the pulse fluctuations of the excimer laser. The light intensity is adjusted so that every particle emits an average of two electrons. The emitted electrons are thermalized by collisions with the gas and attached to the air molecules forming small ions. By applying a small alternating electric field ($E = 500 \text{ V/cm}$; $\nu = 200 \text{ Hz}$), both the electrons and the small ions are removed efficiently because of their high electric mobility [12]. The charged aerosol particles remain unaffected because their electric mobility is at least 2 orders of magnitude lower, compared to the small ions.

In order to measure particle charging the particles are routed into an electrometer where they are removed from the carrier gas with an electrically isolated filter. The deposited charge per unit time is measured by a high sensi-

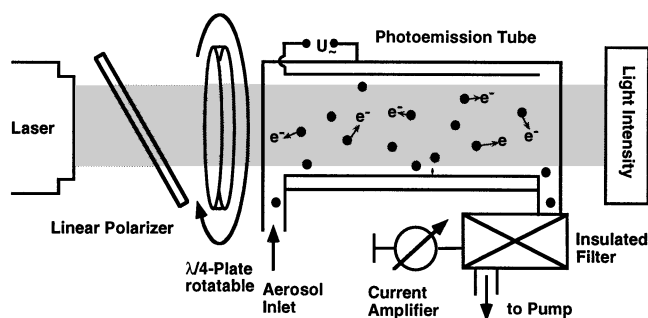


FIG. 2. The photoemission unit. Circularly polarized light illuminates the volume of the photoemission tube and the particles become charged by photoemission. In a subsequent filter the particles are removed and their charge is determined.

tivity current amplifier. Measured currents range between -250 and $+250 \text{ fA}$. The resolution of the electrometer is better than 1 fA and its time constant is 1 sec .

Typical raw data of a measurement are shown in Fig. 3(a). At the beginning the electrometer signal is constant and negative. This is caused by the flow of negatively charged particles from the DMA. After 3 sec the laser fires 20 times and the particles are charged photoelectrically. Consequently the electrometer current becomes positive. Thereafter, the $\lambda/4$ plate is rotated by 90° and the electrometer current decreases exponentially to the starting value. Next, the same procedure is repeated with the opposite circular polarization. Two measured quantities are obtained from the recorded data. The area between the measured curve and the fitted background line is proportional to the total charge of the particles produced by photoemission: $Q^{\text{PE}} = \int I_{\text{electrometer}} dt$. This charge ranges between 0.1 and 10 pC . The constant electrometer signal before and after photoemission corresponds to the particle concentration c_{particle} . From these quantities and the light intensity I_{laser} the normalized photoelectric activity is calculated [18]: $I_{\text{PE}} = Q^{\text{PE}}/(I_{\text{laser}} c_{\text{particle}})$.

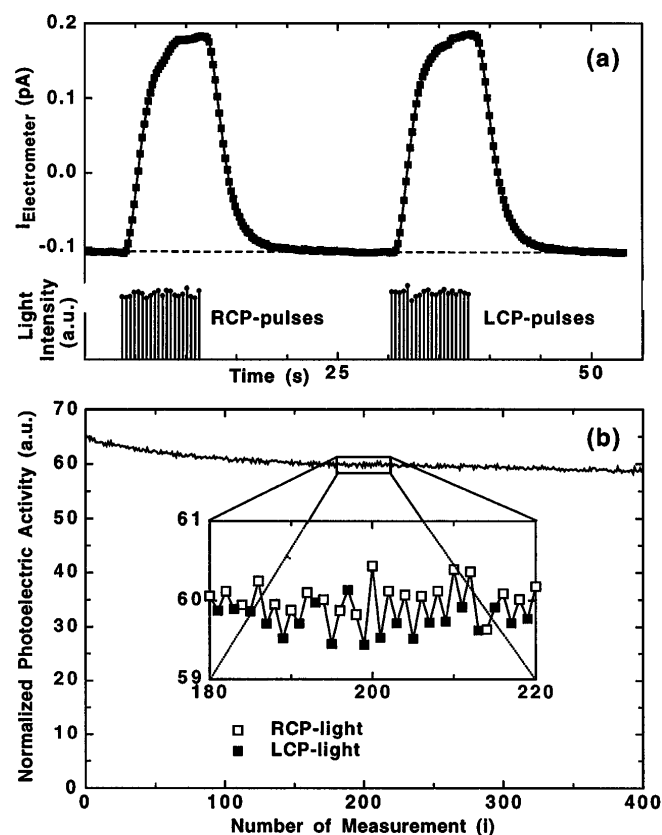


FIG. 3. (a) The charge particle current during one measurement cycle with right and left circularly polarized light. Because of the laser pulses the particles become positively charged. (b) Each data point represents one measurement of the photoelectric charging, normalized to the particle concentration and the light intensity. The zigzag behavior, shown in the inset, is due to the circular dichroism.

Switching the circular polarization and irradiation is typically repeated 200 times. In Fig. 3(b) the normalized photoelectric activities I_{PE}^i of *S*-binaphthalene particles (diameter = 80 nm) are plotted. Measurements with RCP light have even indices i ; those with LCP light have odd indices. It can be seen that the photoelectric activity is almost constant. However, by closer examination a zigzag curve can clearly be observed. This shows that the photoelectric activity of chiral particles depends on the helicity of light.

A set of asymmetries A_i is calculated from the I_{PE}^i by the formula

$$A_i = (-1)^i \frac{I_{PE}^{i+1} - I_{PE}^i}{I_{PE}^{i+1} + I_{PE}^i} = \frac{I_{PE}^{LCP} - I_{PE}^{RCP}}{I_{PE}^{LCP} + I_{PE}^{RCP}}. \quad (1)$$

The A_i are normal distributed as shown below. The average value of the asymmetry is determined to be $-0.2\% \pm 0.01\%$ (experimental standard deviation of the mean). The circular dichroism is observable even with a few measurement cycles. This becomes possible because the resolution of a single measurement is about 0.2%.

In Fig. 4(a) the distribution of the A_i is plotted for both enantiomers. Instead of a histogram a cumulative representation is chosen. The distribution curves of the *R*- and the *S*-enantiomer are clearly separated. While the curve for the *S*-enantiomer is shifted to negative asymmetries the curve for the *R*-enantiomer is shifted to positive values. The asymmetry in photoemission of the *R*-enantiomer is determined to be $0.22 \pm 0.01\%$. This is exactly the inverse value as for the *S*-enantiomer (within the statistical uncertainty) and proves that the observed

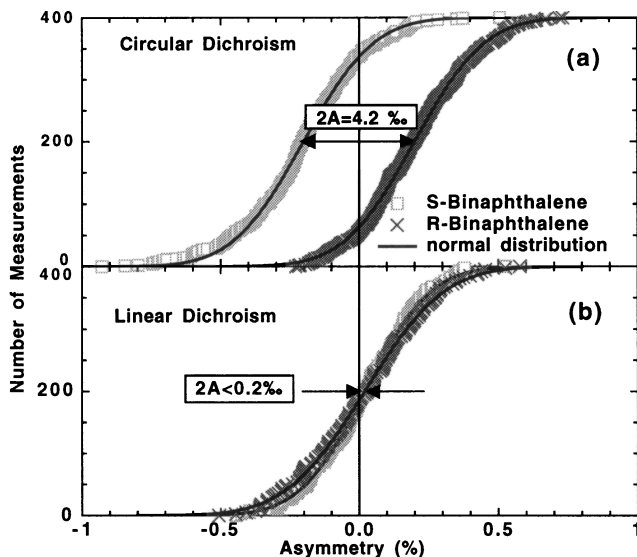


FIG. 4. Distribution curves in a cumulative representation of the measured asymmetries in photoelectric charging. (a) With circularly polarized light a clear distinction of the two enantiomers is seen. (b) No asymmetry is observed when *s*- and *p*-linearly polarized light is used. A normal distribution (solid line) fits the data in all cases.

dichroism in photoemission is not caused by an intrinsic asymmetry in the experiment. Therefore, we conclude that the measured asymmetry is due to the chirality of the particles.

No asymmetry should be seen if linearly polarized light is used. This was checked by the following experiment. A second $\lambda/4$ plate was placed in the optical path. *S*- and *p*-linearly polarized light is now obtained by rotating the first $\lambda/4$ plate exactly in the same way as in the experiments with circularly polarized light. In Fig. 4(b) no significant separation of the distribution curves can be seen. This confirms that the particles in the photoemission tube are not aligned or oriented due to the applied electric field for electron and ion removal.

The circular dichroism in photoemission from a nonoriented system can be described theoretically by an interference term of the electric and the magnetic dipole (E1M1) transition similar to the CD in photoabsorption [6,8]. The magnitude of the interference term scales with kr_{av} compared to the leading dipole transition. Here k is the wave number of the light beam and r_{av} the average radius of the light absorbing orbitals, in our case the π -systems. With the light wavelength of 193 nm and $r_{av} = 0.4$ nm we obtain a scaling factor of 0.65%. This value has to be interpreted as an upper limit. It has to be taken into account that the interference term exists also in the limit of an achiral molecule fixed in space. In the nonchiral case the interference vanishes by summation over all molecule orientations (initial states) and electron emissions directions (final states). For chiral molecules the averaging over all initial and final states cannot result in complete cancellation of the interference term. An incomplete cancellation remains. Therefore asymmetries smaller than 0.5% are expected by time dependent perturbation theory and are confirmed in our experiments.

In Fig. 5 the size dependence of the circular dichroism is shown for particles from both enantiomers. The two curves are mirror symmetric with respect to the zero line. For particles with diameters comparable to the half

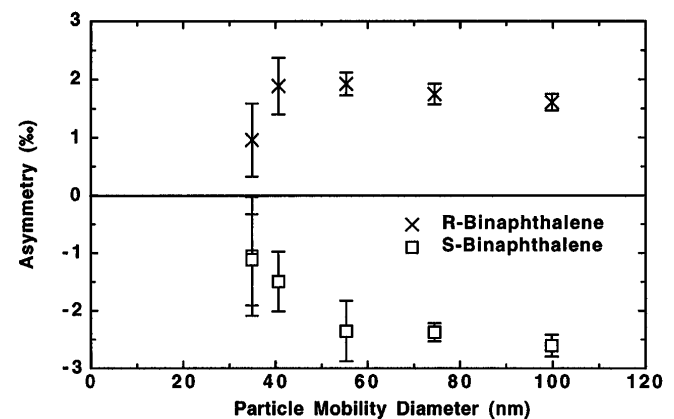


FIG. 5. The measured asymmetries depend on the size of the particles.

wavelength of the light, the asymmetry remains nearly constant. This corroborates the molecular origin of the circular dichroism. For particles with diameters less than 50 nm the asymmetries clearly decrease. This experimental result indicates a structural change in the surface region of the particles. It is reported that the CD in photoabsorption is strongly affected by molecule conformation, which depends on external factors like the solvent used or even the temperature of the solution [3,19]. In our experiment the chiral molecules do not interact with solvent molecules but with identical chiral neighbor molecules. Their interaction should therefore influence the CD in photoemission too. Photoemission experiments on organic particles are mainly sensitive to the particle surfaces and their outermost sublayers [20]. Therefore a slight deformation of the arrangement or of the electronic environment of the chiral molecules in the surface region of the particle can explain the observed size dependence. Such a deformation is expected for small particles where the enhanced curvature leads to an additional surface stress and increases the vapor pressure [21].

In photoemission the absorbed photons are responsible for the dichroism, contrary to the CD in photoabsorption where the extinction of light is measured. In photoabsorption not only the absorbed photons but also the scattered light contribute to the polarization dependence of the extinction coefficients. Dichroism in photoemission is therefore complementary to dichroism in photoabsorption.

We measured the circular dichroism in photoemission of particles consisting of a chiral compound (Fig. 1). The measuring principle is applicable to any chiral particle suspended in a gas. Aerosol particles of biological origin consist of chiral molecules. The detection and rapid assay of bioaerosols is an active field of research [22] and a possible application of the circular dichroism described here.

We thank H.C. Siegmann for proposing the investigation of circular dichroism in aerosols. This work is financially supported by the Swiss National Science Foundation.

[1] *Selected Papers on Natural Optical Activity*, edited by A.

- Lakhtakie (SPIE, Bellingham, WA, 1990).
- [2] L. Pasteur, *Ann. Chim. Phys.* III **24**, 442 (1848).
- [3] *Circular Dichroism and the Conformational Analysis of Biomolecules*, edited by Gerald D. Fasman (Plenum, New York, 1996).
- [4] T. Verbiest, M. Kauranen, Y. V. Rompaey, and A. Persoons, *Phys. Rev. Lett.* **77**, 1456 (1996).
- [5] H. G. Kuball, H. Friesenhan, and A. Schofer, in *Polarized Spectroscopy of Ordered Systems*, edited by B. Samori and E. W. Thulstrup, NATO ASI, Series C, Vol. 242 (Kluwer, Dordrecht, 1988), p. 85.
- [6] B. Ritchie, *Phys. Rev. A* **12**, 567 (1975).
- [7] N. A. Cherepkov, *Chem. Phys. Lett.* **87**, 344 (1982).
- [8] B. Ritchie, *Phys. Rev. A* **13**, 1411 (1976); B. Ritchie, *Phys. Rev. A* **14**, 359 (1976).
- [9] R. L. Dubs, S. N. Dixit, and V. McKoy, *Phys. Rev. Lett.* **54**, 1249 (1985).
- [10] C. Westphal, J. Bansmann, M. Getzlaff, and G. Schönhense, *Phys. Rev. Lett.* **63**, 151 (1989).
- [11] J. Viefhaus *et al.*, *Phys. Rev. Lett.* **77**, 3975 (1996).
- [12] A. Schmitt-Ott, P. Schurtenberger, and H. C. Siegmann, *Phys. Rev. Lett.* **45**, 1284 (1980).
- [13] B. Schleicher, H. Burtscher, and H. C. Siegmann, *Appl. Phys. Lett.* **63**, 1191 (1993); H. Burtscher, *J. Aerosol Sci.* **23**, 549 (1992).
- [14] J. Schiller, H. Lagier, A. Klein, and J. Hormes, *Phys. Scr.* **35**, 463 (1987).
- [15] N. Harada and K. Nakanishi, *Circular Dichroic Spectroscopy, Exciton Coupling in Organic Stereochemistry* (Oxford, Oxford, 1983).
- [16] B. Y. H. Liu and D. Y. H. Pui, *J. Colloid Interface Sci.* **47**, 155 (1974).
- [17] M. Adachi, Y. Kousaka, and K. Okuyama, *J. Aerosol Sci.* **16**, 109 (1985).
- [18] The assumption that the photoelectric charging depends linearly on light intensity was experimentally verified in our experiment. That this assumption holds is not always true in aerosol photoemission.
- [19] J. Sandström, in *Circular Dichroism Principles and Applications*, edited by K. Nakanishi, N. Berova, and R. W. Woody (VHC, New York, 1994), p. 443.
- [20] J. Paul, H. Burtscher, and K. Siegmann, *J. Aerosol Sci.* **26**, Suppl. 1, 239 (1995).
- [21] H. Koehler, *Trans. Faraday Soc.* **32**, 1152 (1936).
- [22] Special issue on *Sampling and Rapid Assay of Bioaerosols* [*J. Aerosol Sci.* **28** (1997)].